# Filtration of Short-Wavelength Light Provides Therapeutic Benefit in Retinitis Pigmentosa Caused by a Common Rhodopsin Mutation

Harry O. Orlans,[1,2] Jonathon Merrill,[3] Alun R. Barnard,[1] Peter Charbel Issa,[1,4] Stuart N. Peirson,[1] and Robert E. MacLaren[1,4]

[1]Nuffield Laboratory of Ophthalmology, University of Oxford, Oxford, United Kingdom
[2]Western Eye Hospital, London, United Kingdom
[3]Biomedical Services, University of Oxford, Oxford, United Kingdom
[4]Oxford Eye Hospital, Oxford, United Kingdom

Correspondence: Harry O. Orlans, Nuffield Laboratory of Ophthalmology, University of Oxford, Levels 5–6 West Wing, John Radcliffe Hospital, Headley Way, Oxford OX3 9DU, UK; enquiries@eye.ox.ac.uk.

Submitted: February 25, 2019
Accepted: May 31, 2019

Citation: Orlans HO, Merrill J, Barnard AR, Charbel Issa P, Peirson SN, MacLaren RE. Filtration of short-wavelength light provides therapeutic benefit in retinitis pigmentosa caused by a common rhodopsin mutation. *Invest Ophthalmol Vis Sci.* 2019;60:2733–2742. https://doi.org/10.1167/iovs.19-26964

**Purpose.** The role of light exposure in accelerating retinitis pigmentosa (RP) remains controversial. Faster degeneration has however been observed in the inferior than superior retina in several forms ("sector" RP), including those caused by the rhodopsin P23H mutation, suggesting a modifying role of incident light exposure in such cases. Rearing of equivalent animal models in complete darkness has been shown to slow the degeneration. Here we investigate the use of red filters as a potential treatment strategy, with the hypothesis that minimizing retinal exposure to light <600 nm to which rods are maximally sensitive may provide therapeutic benefit.

**Methods.** Knockin mice heterozygous for the P23H dominant rhodopsin mutation ($Rho^{P23H/+}$) housed in red-tinted plastic cages were divided at weaning into either untinted or red-tinted cages. Subsequently, photoreceptor layer (PRL) thickness was measured by spectral-domain ocular coherence tomography, retinal function quantified by ERG, and cone morphology determined by immunohistochemical analysis (IHC) of retinal flatmounts.

**Results.** Mice remaining in red-tinted cages had a significantly greater PRL thickness than those housed in untinted cages at all time points. Red housing also led to a highly significant rescue of retinal function as determined by both dark- and light-adapted ERG responses. IHC further revealed a dramatic benefit on cone morphology and number in the red- as compared with the clear-housed group.

**Conclusions.** Limitation of short-wavelength light exposure significantly slows degeneration in the $Rho^{P23H/+}$ mouse model. Red filters may represent a cost-effective and low-risk treatment for patients with rod-cone dystrophy in whom a sectoral phenotype is noted.

Keywords: retinitis pigmentosa, red filter, light, sector, rhodopsin

Several forms of retinitis pigmentosa (RP) demonstrate a more severe degeneration in the inferior than the superior retina. This so-called sector phenotype has been described in association with a large number of dominantly inherited mutations in rhodopsin (*RHO*),[1,2] as well as other genes such as *FAM161A* and *EYS*.[3] It has been proposed that the mechanism for this pattern might, in many cases, be the modifying effect of incident light to which the inferior retina is more intensely exposed.[2,4,5] In support of this hypothesis, rearing of animal models of rhodopsin-related autosomal dominant RP (ADRP), including the $RHO^{P23H}$ transgenic mouse,[6] rat,[7] and *Xenopus laevis*,[8] as well as the $RHO^{T4R}$ dog,[9] in complete darkness has been shown to slow the degenerative process, and such animals appear to have an increased sensitivity to light-induced retinal damage.[6,10] Further, cases of patients with rhodopsin-related ADRP who have degenerative patterns reflective of occupational light exposure have been reported.[1,11] Together, these studies would suggest that a substantial reduction in light exposure might slow the rate of retinal degeneration, and thus be of therapeutic benefit, in patients with sector RP. Although complete occlusion is likely to be most effective in such cases, this has obvious drawbacks as a treatment strategy for clinical application. Given that RP is primarily a rod cell degeneration, and that rods themselves show a more than 50-fold reduction in sensitivity to wavelengths greater than 600 nm,[12,13] it follows that filtration of short-wavelength light may similarly slow the degenerative process while allowing patients to retain useful vision. Only one study has systematically examined the effect of colored lighting and optical filters in an animal model of RP.[14] The authors used rhodopsin levels as a marker of retinal degeneration in the bovine transgenic $Rho^{P23H}$ *X. laevis* model and found evidence supporting a beneficial effect when short-wavelength light was reduced or excluded.

In this study, we explore the effect of filtration of short-wavelength light on the rate of outer retinal degeneration in the $Rho^{P23H/+}$ knockin mouse model of dominant RP,[15] and demonstrate a substantial treatment effect.

## Methods

### Mice and Housing

All animal work was conducted in accordance with the Animals (Scientific Procedures) Act 1986, United Kingdom, and the ARVO Statement for the Use of Animals in Ophthalmic and Vision Research. Mice heterozygous for the *Rho*$^{P23H}$ mutation (henceforth referred to as *Rho*$^{P23H/+}$) were generated by crossing B6.129S6(Cg)-*Rho*$^{tm1.1Kpal}$/J homozygotes[15] obtained from the Jackson Laboratory (Bar Harbor, ME, USA) with C57BL/6J wild-type mice, obtained from Envigo (Huntington, UK). *Rho*$^{P23H/+}$ mice, which additionally carried a green fluorescent protein (GFP) transgene under the control of the neural retina leucine zipper (Nrl) promoter (henceforth referred to as *Nrl-GFP/+*, *Rho*$^{P23H/+}$), were generated by crossing *Rho*$^{P23H/P23H}$ mice with those homozygous for the Tg(Nrl-EGFP)1Asw/J allele (gift from Anand Swaroop, National Eye Institute, Bethesda, MD, USA). Mice carrying a knockout mutation of the X-linked RP GTPase regulator (*Rpgr)* gene (henceforth referred to at *Rpgr*$^{-/y}$)[16] were obtained as a gift from Tiansen Li (NIH, Bethesda, MD, USA). Animals were housed in either clear or red-tinted (tint: RD2A067T) plastic individually ventilated cages (IVCs) of 2.5-mm thickness (Tecniplast, Buguggiate, Italy) in a dedicated facility with a 12-hour light/dark cycle and food and water available ad libitum. Paired clear and red cages housing littermates in any one experiment were positioned in an alternating fashion on the same shelf of the storage rack (second and third from top rows). Animals were randomly allocated to the two different treatment conditions and equal numbers of male and female animals were included for red and clear-housed groups in all experiments. All red IVC changes were performed in a dark room under dim red illumination to avoid exposure of mice to ambient light.

### Spectroradiometry

Readings were taken using a calibrated spectroradiometer (USB2000; Ocean Optics, Dunedin, FL, USA). Transmission spectra for clear and red-tinted IVCs were generated by placing the cage lid between a bright halogen light source and the spectroradiometer detector, and then dividing this value by the signal from the unimpeded light. In situ recordings were acquired by fixing the probe at approximate mouse eye level, pointing forward within cages located within their housing rack. In all cases, measurements were taken at 0.33-nm intervals and data were plotted using a 5-nm boxcar average.

### Retinal Imaging

Retinal imaging was performed using the Spectralis ophthalmic imaging platform (Heidelberg Engineering, Heidelberg, Germany) with a 55° camera lens in a dark windowless room under dim red illumination. En face near infrared (NIR) reflectance images were acquired using the inbuilt confocal scanning laser ophthalmoscope (cSLO), and spectral-domain optical coherence tomography (SD-OCT) was used for cross-sectional imaging of the retina. Mice were anesthetized by intraperitoneal injection of ketamine (Vetalar; Boehringer Ingelheim, Ingelheim am Rhein, Germany, 80 mg/kg body weight) and xylazine (Rompun; Bayer, Leverkusen, Germany, 10 mg/kg body weight). Anesthesia was reversed at the end of procedures by intraperitoneal injection of atipamezole (Antisedan; Zoetis, Parsippany-Troy Hills, NJ, USA, 2 mg/kg body weight). Pupils were dilated using tropicamide 1% and phenylephrine hydrochloride 2.5% applied in sequence (both Minims; Bausch & Lomb, Rochester, NY, USA). Hypromellose 0.3% (Blumont Healthcare, Grantham, UK) was then instilled bilaterally, and polymethyl methacrylate contact lenses (Cantor & Nissel, Brackley, UK) were applied to both eyes and centered over the dilated pupils. Contact lenses served to create a uniform refractive surface for imaging, as well as acting to prevent corneal dehydration, which would otherwise result in the formation of reversible cataract.[17] The SD-OCT imaging protocol consisted of four equally spaced radially orientated scans centered on the murine optic disc. Each image was captured in automatic real-time mode from an average of 25 individual B-scans. Photoreceptor layer (PRL) thickness was measured from these images at mid-peripheral locations (superior, superonasal, nasal, inferonasal, inferior, inferotemporal, temporal, and superotemporal), all at a fixed distance of 22.5° from the optic nerve head, using callipers built in to the Spectralis software. PRL thickness was defined as the vertical distance between the high-contrast outer plexiform layer and retinal pigment epithelium bands seen on the SD-OCT B-scan.[18] Mean PRL thickness for a given mouse was calculated as the mean of all 16 measurements (eight in each eye). All measurements of PRL thickness were conducted blind to treatment condition.

### Electroretinography

Before ERG, mice were dark-adapted overnight (minimum 12 hours) within a purpose-built light-tight cabinet. The procedure was conducted in a designated windowless room with only dim red illumination used during setup where required. Mice were anesthetized and pupils dilated as described above. Animals were then positioned on a heated platform, and ground and reference electrodes inserted subcutaneously on the flank and between the eyes respectively. Custom contact lenses produced from achromatic ACLAR (Honeywell International, Charlotte, NC, USA) were used to hold silver thread Dawson, Trick, and Litzkow (DTL) Plus electrodes (Diagnosys LLC, Cambridge, UK) in place on each cornea. The platform was then maneuvered so that the mouse was located centrally within a Ganzfeld stimulator (Colordome; Diagnosys LLC, Cambridge, UK). The ERG protocol was undertaken using an Espion E3 system (Diagnosys LLC), and consisted of dark- and light-adapted phases. In the dark-adapted phase, responses were elicited by brief uniform flashes of white light of intensity ranging from –6 to 1.4 log cd.s/m$^2$, increasing in log unit steps. At each luminance level, up to 16 recordings were taken that were subsequently averaged. After completion of the dark-adapted phase, animals were light-adapted using a full-field white light of 30 cd/m$^2$ for 10 minutes. The light-adapted phase then consisted of bright white flashes superimposed on this background. The intensity of these stimuli increased in half log unit steps from 0.3 to 10 cd.s/m$^2$, with each measurement taken as an average of 25 individual recordings. Repeated measures 2-way ANOVA tests, with housing type and stimulus intensity as factors, were used to compare responses between red- and clear-housed groups.

### Immunohistochemistry

Retinal flat mount processing and staining for cone arrestin were conducted following completion of ERG in accordance with a previously published protocol.[19] The LSM-710 inverted confocal microscope system (Zeiss, Oberkochen, Germany) was used to image the resulting specimens.

### *Rpe65* Polymorphism Genotyping

Genomic DNA was extracted from ear notch tissue by alkaline lysis. *Rpe65* polymorphism genotyping of these samples was

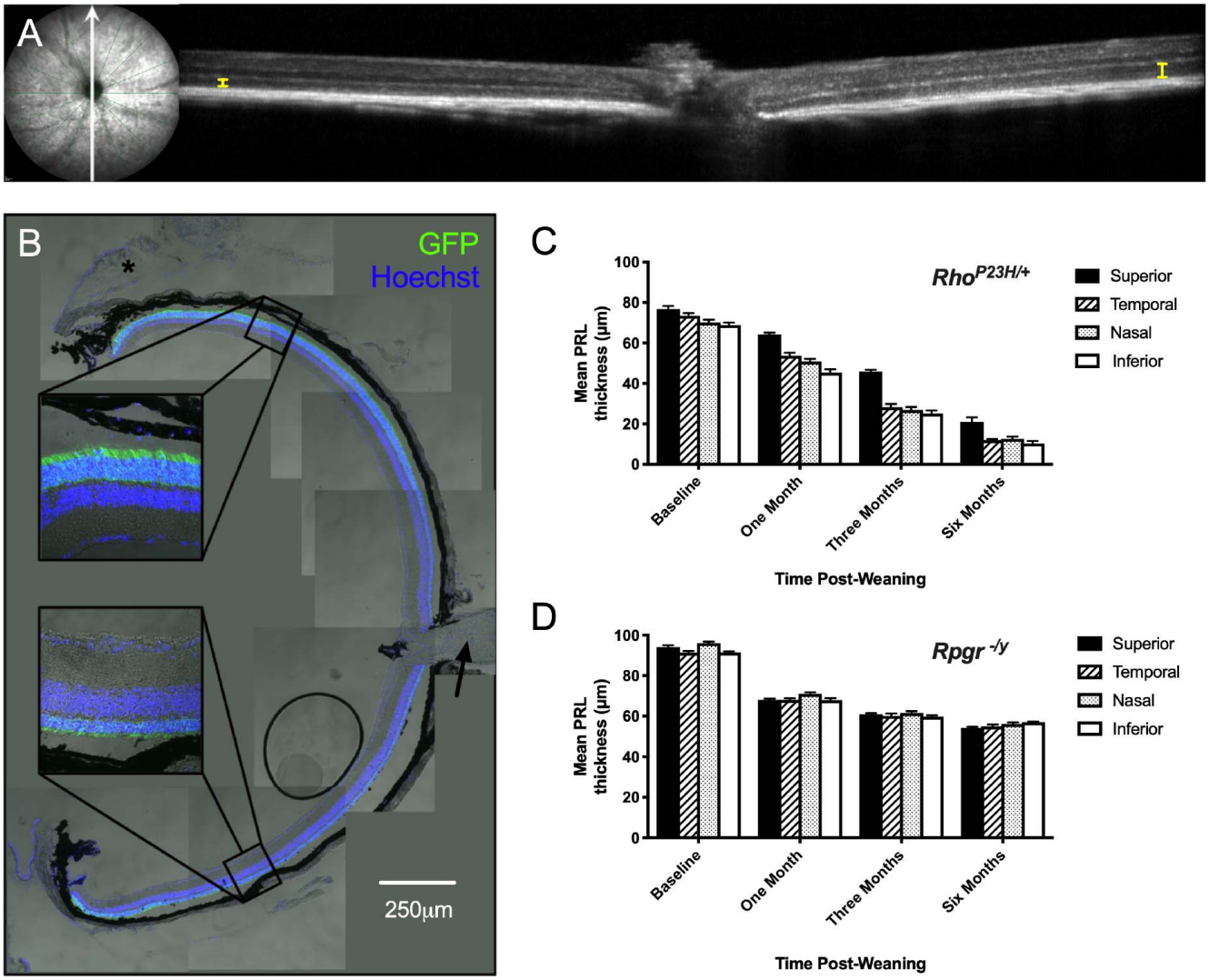


**Figure 1.** The inferior retina degenerates more rapidly than the superior retina in the *Rho*$^{P23H/+}$ but not in the *Rpgr*$^{-/y}$ mouse model of RP. (**A**) Vertical SD-OCT retinal image from a *Rho*$^{P23H/+}$ mouse aged 3 months. The *white arrow* through the accompanying en face infrared cSLO fundus image indicates the orientation of the section. *Yellow callipers* at the inferior and superior aspects of the section indicate the PRL at these locations. (**B**) Vertical cryosection through an *Nrl.GFP/+*, *Rho*$^{P23H/+}$ mouse eye aged 3 months. The superior rectus muscle is marked with a *black asterisk* and the optic nerve is indicated by a *black arrow*. Rod photoreceptors express GFP in this model highlighting the outer nuclear layer and inner segments in *green*. (**C**, **D**) Mean photoreceptor layer (PRL) thickness ± SEM by retinal quadrant as a function of time post-weaning for *Rho*$^{P23H/+}$ (**C**; $n = 9$) and *Rpgr*$^{-/y}$ (**D**; $n = 9$) mice. The superior PRL thickness was significantly greater than that of all other retinal quadrants in the *Rho*$^{P23H/+}$ model and this difference increased over time (repeated measures 2-way ANOVA with factors of retinal quadrant and time: $F_{3,24} = 336.1$, $P < 0.0001$ for effect of retinal quadrant; $F_{9,72} = 13.08$, $P < 0.0001$ for interaction time × retinal quadrant; $P = 0.0001$ for superior versus temporal, nasal and inferior retinal quadrants, Sidak's multiple comparison test). No superior-inferior difference in PRL thickness was detected in *Rpgr*$^{-/y}$ mice ($P = 0.88$, Sidak's multiple comparison test).

then performed as per the PCR restriction length polymorphism method described by Kim et al.,[20] using forward and reverse primers 5′-ACCAGAAATTTGGAGGGAAAC and 5′-CCCTTCCATTCAGAGCTTCA, respectively.

## Results

### Regional Variation in Retinal Degeneration of RP Models

*Rho*$^{P23H/+}$ mice reared in standard clear cages were found by SD-OCT to have a thicker PRL superiorly than in the nasal, temporal, and inferior retinal quadrants ($P = 0.0001$ in all cases; Fig. 1). At postnatal day (PND) 21, this difference was small but statistically significant. With advancing age, the difference in PRL thickness between superior and temporal, nasal, and inferior quadrants increased. This would suggest that the superior retina degenerates more slowly in this model (Fig. 1C). This superior-inferior difference was also confirmed histologically in the *Nrl-GFP/+*, *Rho*$^{P23H/+}$ mouse in which GFP is expressed in rods under the control of the *Nrl* promoter (Fig. 1B). By contrast, the PRL thickness of the superior retina was not significantly different from that of the inferior retina in either wild-type mice ($P = 0.15$; data not shown) or in the *Rpgr*$^{-/y}$ mouse model of X-linked RP as measured by SD-OCT ($P = 0.88$; Fig. 1D).

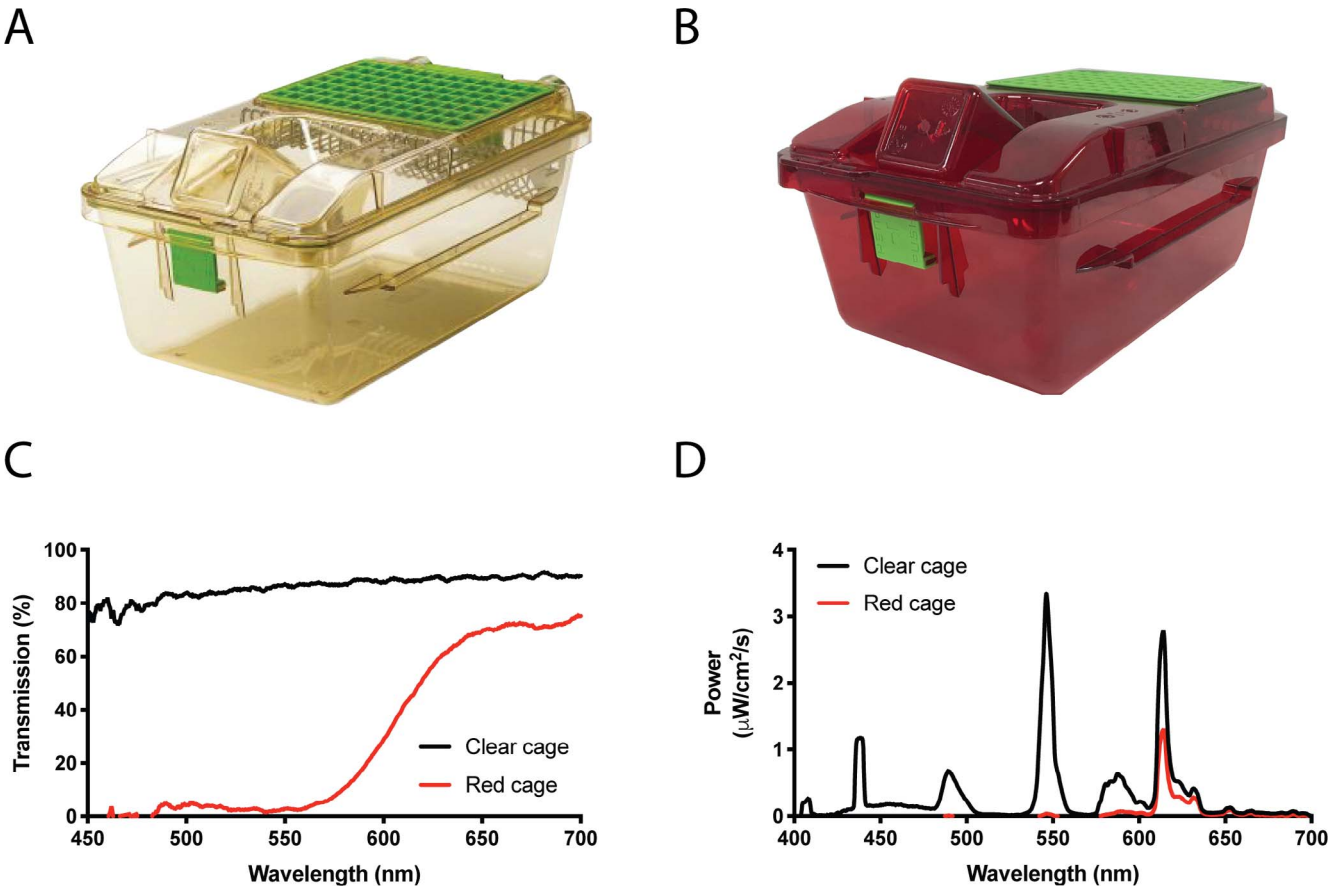


FIGURE 2. IVCs. (**A**) Standard clear IVC. (**B**) Red-tinted IVC (Tecniplast). Both cage types include a white filter located on the posterior upper surface beneath a green plastic retainer. (**C**) Transmission spectra recorded for clear and red-tinted IVCs using a halogen light source. Recordings below 450 nm are not plotted, as halogen lights emit very little light in this part of the visible spectrum giving an unfavorable signal-to-noise ratio. (**D**) Spectral distribution for both cage types recorded from within cages located in situ in the animal housing facility under fluorescent lighting.

## Red IVCs Filter Short-Wavelength Light

Figure 2C shows the transmission spectra of clear and red-tinted IVCs recorded using a bright halogen light source. Absolute light measurements for the two cage types recorded in situ under fluorescent lighting are shown in Figure 2D. Note that the red tint results in the near complete attenuation of all peaks below 600 nm with a significant reduction of the peak at 614 nm. Thus, red IVCs used here appear to act as long-pass light filters, significantly attenuating light transmission for wavelengths below approximately 600 nm. Total absolute light levels recorded in situ were 659 lux for clear IVCs and 92 lux for red IVCs. The predicted effect of the tint on activation of the four mouse photopigments (rhodopsin, melanopsin, and short-/long-wavelength cone opsins) was calculated using the formulae described by Lucas et al.[21] in their irradiance toolbox, and is shown in Supplementary Figure S1.

## Rearing Within Red IVCs Slows Retinal Degeneration in the *Rho*$^{P23H/+}$ Model

*Rho*$^{P23H/+}$ pups born within red IVCs were divided at postnatal week (PNW) 3 into clear or red-tinted IVCs. PRL thickness was subsequently measured by SD-OCT 1, 3, and 6 months later, and retinal function determined by ERG 6 months after weaning. Mean PRL thickness as measured by SD-OCT was significantly greater for animals housed in red-tinted IVCs than in those housed in standard conditions at all time points examined (repeated-measures 2-way ANOVA with factors of cage type and time post-randomization: $F_{1,20} = 68.03$, $P < 0.0001$ for effect of cage type; $F_{3,60} = 29.61$, $P < 0.0001$ for interaction cage type × time; Fig. 3).

The inferior:superior ratio of PRL thickness was significantly greater for the red-housed group throughout the experiment, indicating a relative attenuation of the sectoral phenotype in these animals ($P = 0.001$; Supplementary Fig. S2).

ERG performed 6 months after weaning showed a greater preservation of both dark- and light-adapted responses in the red IVC group than in the clear IVC group (Fig. 4).

In a similar fashion, *Rpgr*$^{-/y}$ pups born within red IVCs were divided at PNW3 into clear or red-tinted IVCs, and PRL thickness measured by SD-OCT after 1, 3, and 6 months. In contrast to the *Rho*$^{P23H/+}$ model, no significant difference in PRL thickness was observed between red and clear-housed groups at any time point ($P = 0.90$; Supplementary Fig. S3).

## Red Filters Lead to a Relative Preservation of Cone Morphology in the *Rho*$^{P23H/+}$ Model

Following ERG, *Rho*$^{P23H/+}$ mice that had been housed in red or clear IVCs were culled and eyes extracted. The retinas were immunostained for cone arrestin and flat-mounted for en face confocal fluorescence microscopy. Cones from animals housed in clear cages had disrupted pedicles, shortened axons, and fewer and more disorganized outer segments (Fig. 5). Their red IVC housed littermates displayed cone anatomy that was closer in appearance to that observed in age-matched wild-type

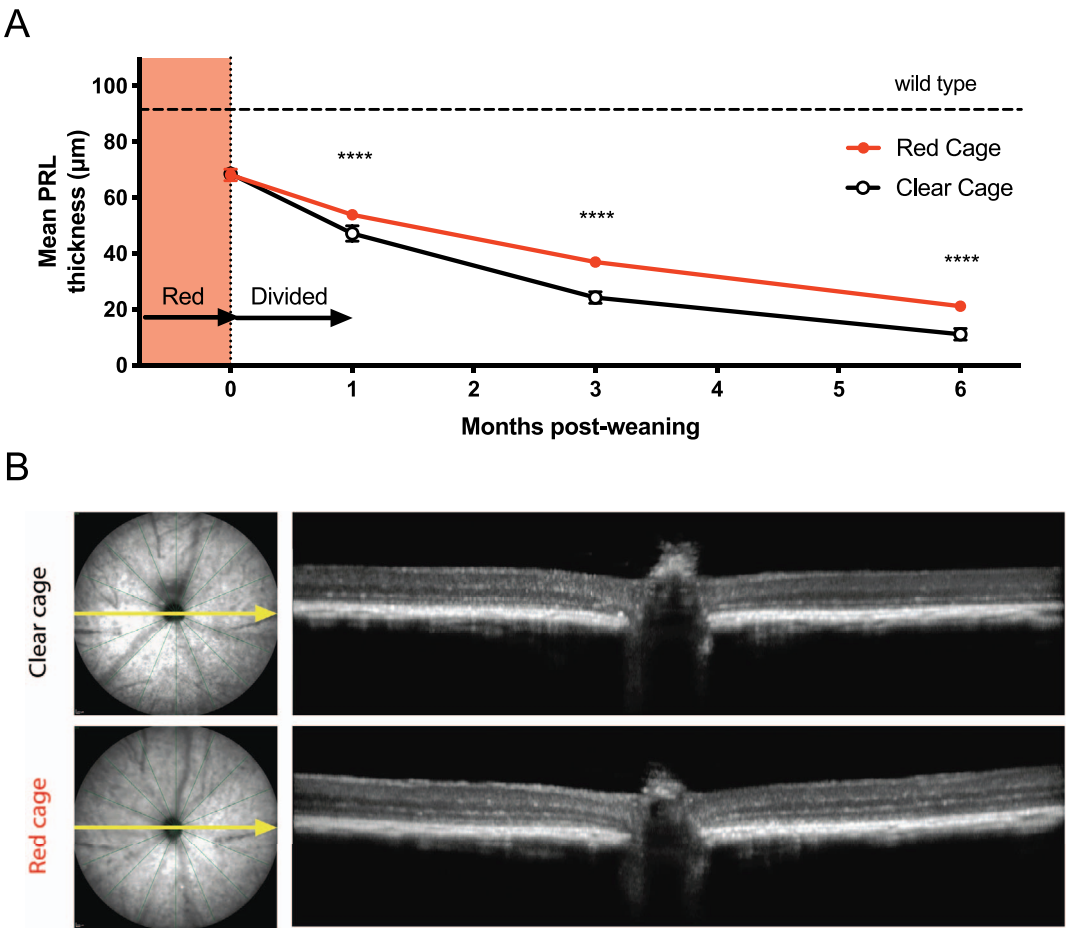


Figure 3. Rearing in red IVCs slows the rate of outer retinal degeneration in the $Rho^{P23H/+}$ mouse as measured by SD-OCT. Animals born in red IVCs were divided between clear and red IVCs at the point of weaning on PND21. (**A**) Mean PRL thickness recorded by SD-OCT. *Error bars* represent the 95% confidence interval about the mean. For points where no error bar is displayed, the confidence interval is smaller than the size of the symbol. The *dashed horizontal line* represents the mean PRL thickness measured from four C57BL/6J wild-type mice at 6 months post-weaning. $^{****}P < 0.0001$, Sidak's multiple comparison test. (**B**) Representative NIR reflectance images and horizontal SD-OCTs for littermates housed in clear and red IVCs. The particular cross-section displayed is indicated by the *yellow arrow* in the corresponding en face NIR reflectance image.

animals. Long-term housing in red IVCs thus resulted in a relative preservation of cone morphology.

### Effect of Switching Adult $Rho^{P23H/+}$ Mice Reared Under Standard Conditions into Red IVCs

To determine whether slowing of retinal degeneration in the $Rho^{P23H/+}$ mouse could be achieved when red filters are applied at more advanced stages of disease, further cohorts reared under standard conditions were divided between the two cage types at weaning (i.e., PNW3; $n = 8$ per group) and 1 month after weaning (at which point PRL thickness was already reduced to approximately 60% of that of wild-type animals; $n = 10$ in red group, $n = 9$ in clear group). A small but significant benefit on PRL thickness was observed in the group of animals switched from clear into red IVCs at weaning compared with those remaining within standard conditions ($P = 0.0002$; Fig. 6A). No difference in PRL thickness was, however, detected between the two groups divided at PNW7 ($P = 0.71$; Fig. 6B). These results would suggest that early intervention may be required to see a treatment effect associated with filtration of short-wavelength light in the $Rho^{P23H/+}$ mouse model.

### *Rpe65* L450M Polymorphism Status of $Rho^{P23H/+}$ Mice

The L450M polymorphism within the *Rpe65* gene is known to influence susceptibility of the mouse retina to light-induced damage,[22] with strains with the leucine variant appearing more vulnerable.[20,23] $Rho^{P23H/+}$ mice were genotyped according to the restriction fragment length polymorphism assay described by Kim et al.[20] to determine whether presence of the leucine variant (rather than, or in addition to, the P23H rhodopsin mutation) could be responsible for the observed effect of light on the retinal degenerative phenotype. All $Rho^{P23H/+}$ mice genotyped by this method were found to be homozygous for the methionine variant of *Rpe65* (Supplementary Fig. S4). L450M polymorphism of *Rpe65* cannot therefore explain the sector phenotype observed in $Rho^{P23H/+}$ mice.

## Discussion

Long-term housing within red-tinted IVCs resulted in a significant slowing of the rate of degeneration in the $Rho^{P23H/+}$ retina, which has a superior-inferior difference in PRL thickness, but not in the $Rpgr^{-/y}$ model of RP that demon-

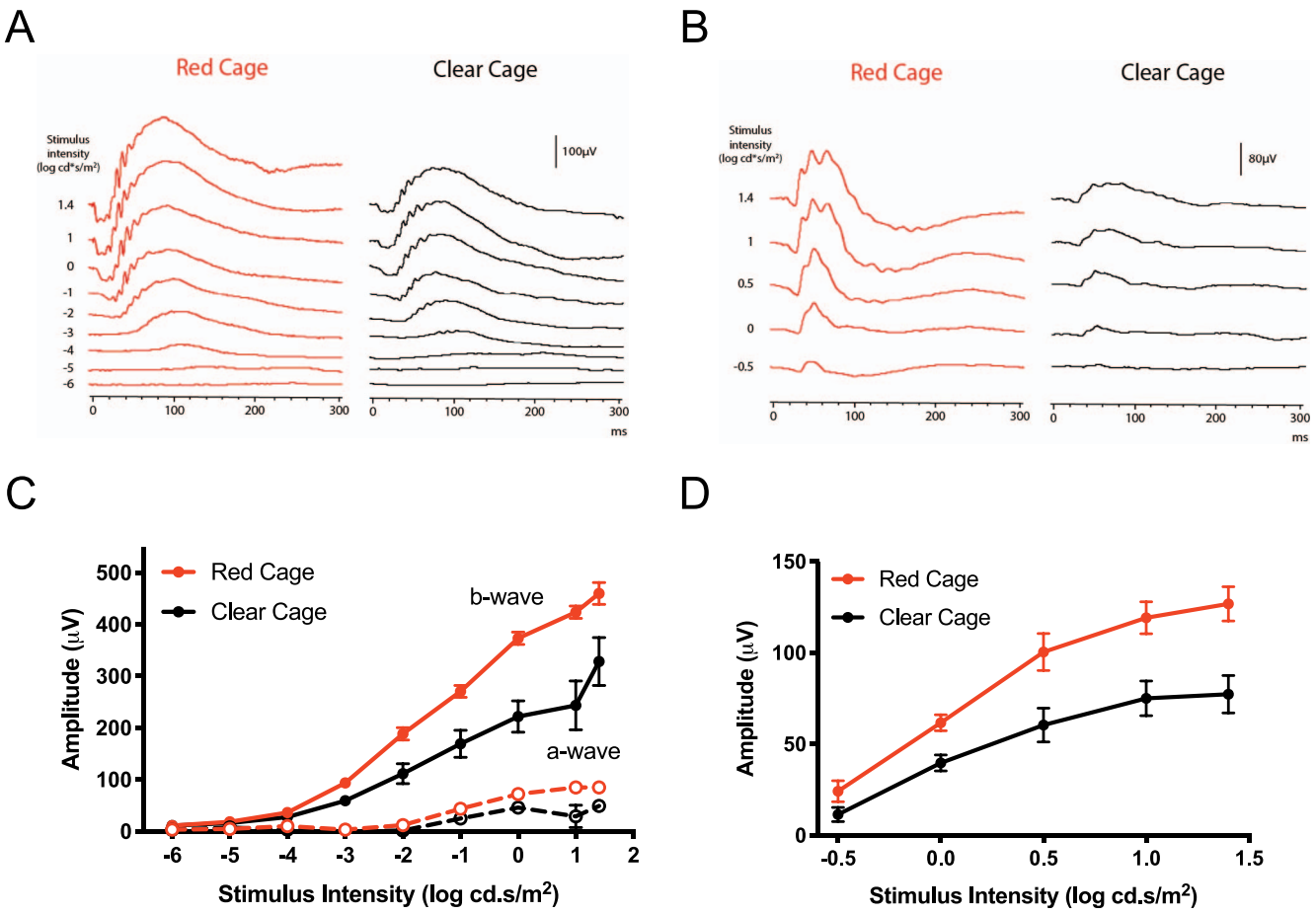


**Figure 4.** ERG recordings demonstrate a relative preservation of retinal function in red-housed animals when compared with their clear-housed littermates. (**A**) Representative dark-adapted traces. (**B**) Representative light-adapted traces. (**C**) Dark-adapted ERG irradiance-response curves (mean response ± SEM); a- and b-wave responses are represented by *dashed* and *solid lines*, respectively. Repeated measures 2-way ANOVA for effect of housing: $F_{1,18} = 18.13$, $P = 0.0005$ for a-wave; $F_{1,18} = 12.95$, $P = 0.002$ for b-wave. (**D**) Light-adapted ERG irradiance response curves (mean response ± SEM). Repeated measures 2-way ANOVA for effect of housing: $F_{1,18} = 12.13$, $P = 0.003$.

strates no such difference. A sector pattern of photoreceptor loss has been described in dominant RP caused by a variety of missense mutations in the rhodopsin gene.[1,2,24–30] These mutations, which appear to confer a light-sensitive degenerative phenotype, are those associated with misfolding and endoplasmic reticulum (ER) retention, and those with altered posttranslational modification and reduced stability of the protein.[5,31] Potential mechanisms by which light might act as a modifying factor include depletion of free 11-*cis*-retinal, which in low-luminance conditions may act as a molecular chaperone for rhodopsin,[8,14,15] direct destabilization of the mutant protein within the rod outer segment,[2,32,33] and via activation of the phototransduction cascade.[15,34] Interestingly, misfolded mutant opsin does not appear to induce upregulation of the proapoptotic PERK pathway in the P23H knockin mouse.[35] Recent evidence also has suggested a role for autophagy induced by the misfolded protein in the mechanism of photoreceptor death in this model.[36] The red IVCs used here acted as long-pass light filters to substantially impede transmission of light of wavelength below 600 nm. Given that the peak spectral sensitivities of free 11-*cis*-retinal and chromophore-bound rhodopsin are approximately 370 to 400 nm and 495 to 510 nm, respectively,[14] it follows that such filters should at least be partially effective, regardless of whether the mechanism underlying light-induced damage is mutant rhodopsin activation, chromophore depletion, stimulation of phototransduction, or a combination of the above.

Although no rescue effect was demonstrated as a result of red-tinted housing in the $Rpgr^{-/y}$ mouse in this study, similar investigation in other relevant animal models, such as the $Rho^{D190N/+}$ knockin mouse[37] and the light-sensitive $RHO^{T17M}$ transgenic mouse,[38] would be of significant interest.

In this study, the observed treatment effect was diminished when red filters were applied to animals later in the course of the disease (Fig. 6). It is possible that ER accumulation of mutant opsin by this time may have been so great that the additional availability of 11-*cis*-retinal was insufficient to affect the fate of individual photoreceptors. Indeed, upregulation of proteins associated with the unfolded protein response and cell death has been detected as early as PND30 in mice heterozygous for the P23H mutation.[35] It is, however, difficult to establish the extent to which these findings can be applied to patients with equivalent rhodopsin mutations in whom, unlike the $Rho^{P23H/+}$ mouse model, disease progression is typically slow.[15,39]

Housing of mice within red IVCs was associated with a significant reduction in the observed altitudinal gradient of retinal degeneration (Supplementary Fig. S2). This gradient was not, however, completely abolished. It is conceivable that a greater treatment effect might be achieved if long-pass filters with higher cutoff wavelengths were to be used, as has been

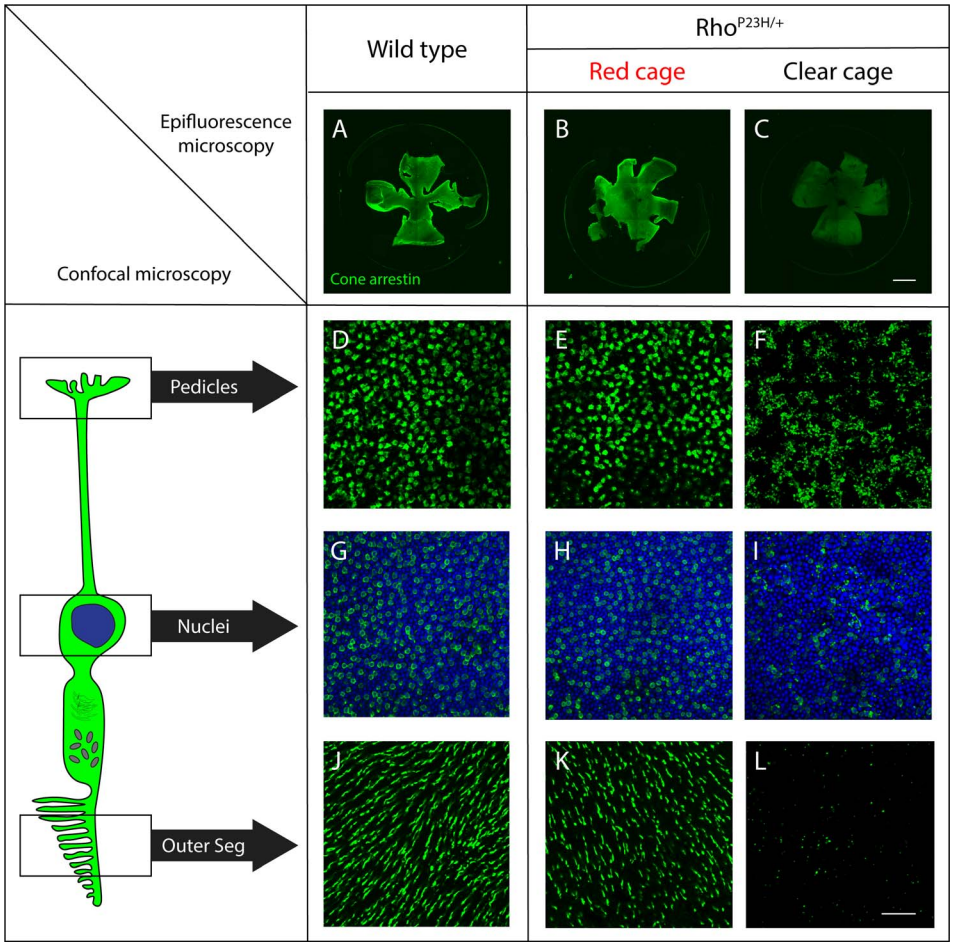


**Figure 5.** Rearing within red IVCs results is a relative preservation of cone morphology. Retinas from animals aged 6 months post-weaning were harvested, stained for cone arrestin (shown in *green*) and flat-mounted for microscopy. (**A–C**) A brighter signal was seen on low-power epifluorescence microscopy for *Rho*$^{P23H/+}$ animals housed in red cages (**B**) than for their littermates housed in standard clear cages (**C**), with the staining pattern in the red-housed group appearing more similar to that observed in age-matched wild-type controls (**A**). *Scale bar*: 2 mm. (**D–L**) En face confocal fluorescence microscopy. Photoreceptor nuclei are stained with Hoechst 33342 nuclear stain (*blue*). Cone arrestin staining of retinas from clear-housed *Rho*$^{P23H/+}$ mice revealed disrupted pedicles (**F**), fewer nuclei (**I**), and loss of outer segments (**L**). These anatomical features for their red-housed littermates (**E**, **H**, **K**) were again more similar to those observed in age-matched wild-type controls (**D**, **G**, **J**). *Scale bar*: 10 µm.

demonstrated previously in the transgenic *RHO*$^{P23H}$ tadpole model.[14]

Short-wavelength light-filtering IVCs were associated with a relative preservation of cone morphology as determined by immunofluorescence confocal microscopy (Fig. 5), and of cone function as quantified by light-adapted ERG (Fig. 4). Cones die in RP secondary to rod death, and it is this change that ultimately results in the symptomatic constriction of the visual field in photopic light conditions, and eventual loss of central acuity.[40,41] Degeneration of rods in RP reduces outer retinal oxygen consumption and leads to high levels of oxygen in the surviving tissue.[42] This is thought to trigger cone death through a mechanism of oxidative stress.[41] Reduced levels of rod-derived cone viability factor, an inactive thioredoxin secreted by rods, which protects cones from oxidative stress,[43] also may contribute. The relative conservation of cone structure and function observed here likely reflects a delay in the onset of secondary cone death that resulted from a slowing of rod degeneration for animals housed in red cages. Thus, it is possible that long-term use of red optical filters might allow prolonged retention of useful photopic vision in patients with light-sensitive sector RP. Reasonable tolerability of such red-tinted optical lenses has been reported among RP patients, with many users reporting acceptable cosmetic appearance, increased ocular comfort, and improved visual performance.[44]

We cannot exclude the possibility that the treatment effect observed in this study resulted from a general reduction in overall light exposure induced by the red tint (Fig. 2D). Indeed, a similar degree of photoreceptor preservation might be achievable with highly attenuating neutral density filters. Red optical filters, however, have the advantage of preserving visual function under ambient light conditions. There are a number of predictable disadvantages associated with the short- and long-term clinical use of red-tinted optical filters as a treatment strategy for light-sensitive RP that must be considered. First, color discrimination would undoubtedly be affected owing to a substantial reduction in the stimulation of S-cones, and to a lesser extent M-cones (Supplementary Fig. S1). This would be expected to produce a tritan-like color vision abnormality. Some patients may also dislike seeing the world with a red tint. Studies in healthy subjects have, however, demonstrated that plasticity of color perception occurs in response to the extended use of colored optical filters, suggesting that these perceptual changes may diminish over time.[45] Second, it is conceivable that nyctalopia, already a cardinal symptom in RP, may be exacerbated by the reduction in rod activation consequent on filtration of short-wavelength light. The extent

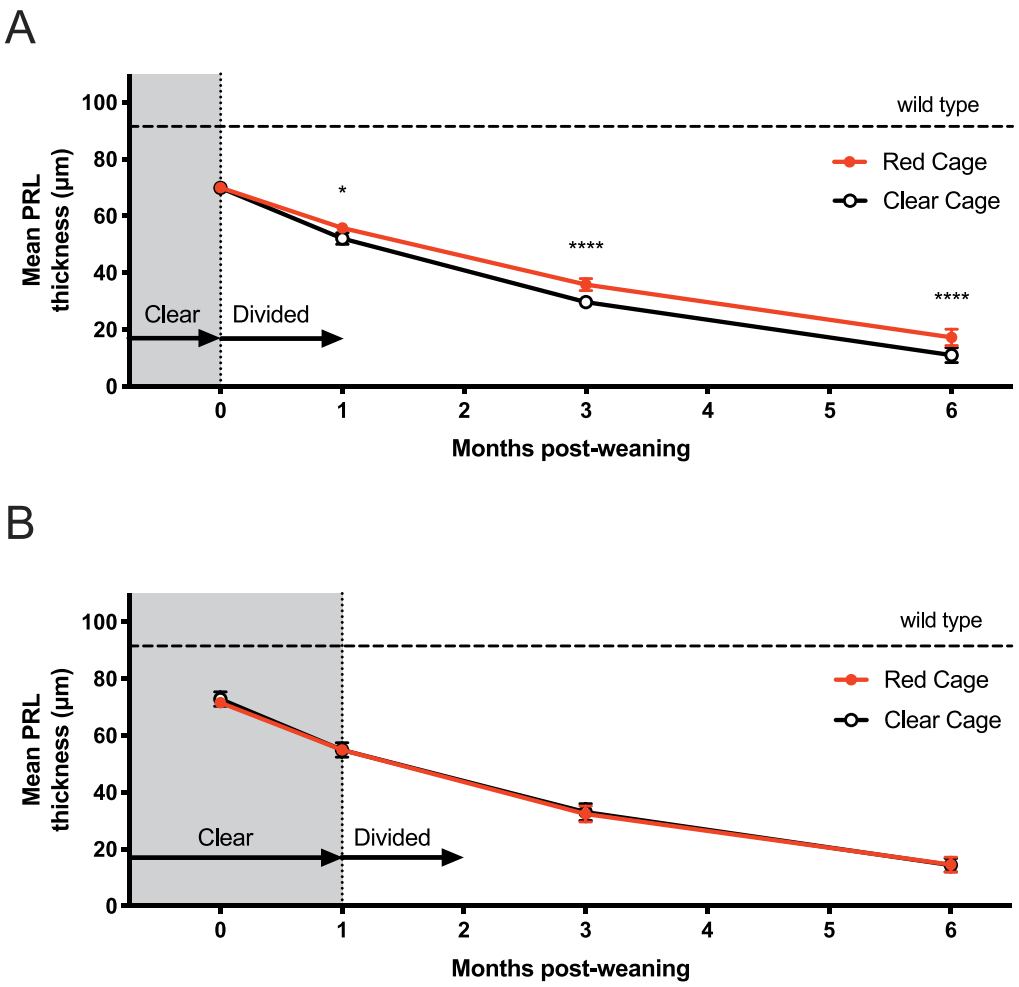


**Figure 6.** Moving $Rho^{P23H/+}$ mice reared in standard conditions into red IVCs after increasing periods of time is associated with a reduction in the associated treatment effect. $Rho^{P23H/+}$ mice were born and initially reared within standard clear cages and were divided between clear and red IVCs at the times indicated by *vertical dotted lines*. *Error bars* represent the 95% confidence interval about the mean. The *dashed horizontal line* represents the mean PRL thickness measured from four C57BL/6J wild-type mice at 6 months post-weaning. (**A**) Cohort divided between cage types at weaning (PNW3); $n = 8$ per group. Repeated measures 2-way ANOVA with factors of cage type and time post-randomization: $F_{1,14} = 23.81$, $P = 0.0002$ for effect of cage type; $F_{3,41} = 8.87$, $P = 0.0001$ for interaction cage type × time; $^{*}P < 0.05$, $^{****}P < 0.0001$, Sidak's multiple comparison test. (**B**) Cohort divided between cage types at 1 month post-weaning (PNW7); $n = 10$ in red group, $n = 9$ in clear group. Repeated measures 2-way ANOVA with factors of cage type and time post-randomization: $F_{1,17} = 0.14$, $P = 0.71$ for effect of cage type.

to which this occurs would have to be determined experimentally. In scotopic environments, the benefit conferred by red-tinted spectacles would, however, be marginal, and they could simply be removed by the patient if found to be troublesome. Third, red filters would be expected to lead to a substantial reduction in activation of retinal melanopsin, which has a peak spectral sensitivity of approximately 479 nm.[46] Intrinsically photosensitive retinal ganglion cells express this photopigment and, through their projection to the suprachiasmatic nucleus of the hypothalamus, play a key role in the entrainment of normal sleep-wake cycles and circadian rhythms.[47] Indeed, sleep disturbance has been demonstrated in patients with advanced nuclear sclerotic-type cataracts, which act as yellow-tinted optical filters and thus absorb light in the blue part of the visible spectrum.[48–50] The melanopsin system may, however, be capable of adaptation in response to chronic changes in light spectral composition. Evidence for this comes from a study by Giménez and colleagues,[51] which showed that the acute reduction in the melatonin-suppressing effect of light observed after the application of soft orange-tinted contact lenses normalized after approximately 2 weeks of continuous use in healthy subjects. Red filters may not, therefore, have a substantial impact on sleep and circadian function when applied continuously, although patients would have to be closely monitored for related symptoms in any future clinical trial.

In summary, we have demonstrated relative rescue of a relevant mouse model of dominant rhodopsin-related sector RP using long-pass light filters. Red filters in the form of tinted spectacles or contact lenses might represent a low-cost and low-risk intervention to slow the rate of photoreceptor loss in patients with sector RP. Before any future clinical trial, it would be important to establish the short- and long-term effects of red filters on visual acuity, contrast sensitivity, color perception, and their overall tolerability in healthy volunteers and in RP patients.

## *Acknowledgments*

The authors thank all of the animal technicians involved in maintaining the mice used in this study under strict light conditions. They also thank the MRC and Fight for Sight for providing the required financial support.

Supported by MRC/Fight for Sight, Grant reference: MR/N00101X/1.

Disclosure: **H.O. Orlans**, None; **J. Merrill**, None; **A.R. Barnard**, None; **P. Charbel Issa**, None; **S.N. Peirson**, None; **R.E. MacLaren**, None

## *References*

1. Heckenlively JR, Rodriguez JA, Daiger SP. Autosomal dominant sectoral retinitis pigmentosa: two families with transversion mutation in codon 23 of rhodopsin. *Arch Ophthalmol*. 1991; 109:84–91.
2. Ramon E, Cordomi A, Aguilà M, et al. Differential light-induced responses in sectorial inherited retinal degeneration. *J Biol Chem*. 2014;289:35918–35928.
3. Verbakel SK, van Huet RAC, Boon CJF, et al. Non-syndromic retinitis pigmentosa. *Prog Retin Eye Res*. 2018;66:157–186.
4. Paskowitz DM, LaVail MM, Duncan JL. Light and inherited retinal degeneration. *Br J Ophthalmol*. 2006;90:1060–1066.
5. Athanasiou D, Aguila M, Bellingham J, et al. The molecular and cellular basis of rhodopsin retinitis pigmentosa reveals potential strategies for therapy. *Prog Retin Eye Res*. 2017; 62:1–23.
6. Naash ML, Peachey NS, Li XZ, et al. Light-induced acceleration of photoreceptor degeneration in transgenic mice expressing mutant rhodopsin. *Invest Ophthalmol Vis Sci*. 1996;37:775–782.
7. Organisciak DT, Darrow RM, Barsalou L, Kutty RK, Wiggert B. Susceptibility to retinal light damage in transgenic rats with rhodopsin mutations. *Invest Ophthalmol Vis Sci*. 2003;44: 486–492.
8. Tam BM, Moritz OL. Dark rearing rescues P23H rhodopsin-induced retinal degeneration in a transgenic. *Neurobiol Dis*. 2007;27:9043–9053.
9. Iwabe S, Ying GS, Aguirre GD, Beltran WA. Assessment of visual function and retinal structure following acute light exposure in the light sensitive T4R rhodopsin mutant dog. *Exp Eye Res*. 2016;146:341–353.
10. Walsh N, Van Driel D, Lee D, Stone J. Multiple vulnerability of photoreceptors to mesopic ambient light in the P23H transgenic rat. *Brain Res*. 2004;1013:194–203.
11. Iannaccone A, Man D, Waseem N, et al. Retinitis pigmentosa associated with rhodopsin mutations: correlation between phenotypic variability and molecular effects. *Vision Res*. 2006;46:4556–4567.
12. Bowmaker J, Dartnall H. Visual pigments of rods and cones in a human retina. *J Physiol*. 1980;298:501–511.
13. Govardovskii VI, Fyhrquist N, Reuter TOM, Kuzmin DG, Donner K. In search of the visual pigment template. *Vis Neurosci*. 2000;17:509–528.
14. Tam BM, Qazalbash A, Lee HC, Moritz OL. The dependence of retinal degeneration caused by the rhodopsin P23H mutation on light exposure and vitamin a deprivation. *Invest Ophthalmol Vis Sci*. 2010;51:1327–1334.
15. Sakami S, Maeda T, Bereta G, et al. Probing mechanisms of photoreceptor degeneration in a new mouse model of the common form of autosomal dominant retinitis pigmentosa due to P23H opsin mutations. *J Biol Chem*. 2011;286:10551–10567.
16. Hong DH, Pawlyk BS, Shang J, Sandberg MA, Berson EL, Li T. A retinitis pigmentosa GTPase regulator (RPGR)-deficient mouse model for X-linked retinitis pigmentosa (RP3). *Proc Natl Acad Sci U S A*. 2000;97:3649–3654.
17. Issa PC, Singh MS, Lipinski DM, et al. Optimization of in vivo confocal autofluorescence imaging of the ocular fundus in mice and its application to models of human retinal degeneration. *Invest Ophthalmol Vis Sci*. 2012;53:1066–1075.
18. Staurenghi G, Sadda S, Frcophth UC, et al. Proposed lexicon for anatomic landmarks in normal posterior segment spectral-domain optical coherence tomography. The IN OCT Consensus. *Ophthalmology*. 2014;121:1572–1578.
19. Hassall MM, Barnard AR, Orlans HO, et al. A novel achromatopsia mouse model resulting from a naturally occurring missense change in Cngb3. *Invest Ophthalmol Vis Sci*. 2018;59:6102–6110.
20. Kim SR, Fishkin N, Kong J, Nakanishi K, Allikmets R, Sparrow JR. Rpe65 Leu450Met variant is associated with reduced levels of the retinal pigment epithelium lipofuscin fluorophores A2E and iso-A2E. *Proc Natl Acad Sci U S A*. 2004;101: 11668–11672.
21. Lucas RJ, Peirson SN, Berson DM, et al. Measuring and using light in the melanopsin age. *Trends Neurosci*. 2014;37:1–9.
22. Danciger M, Matthes MT, Yasamura D, et al. A QTL on distal Chromosome 3 that influences the severity of light-induced damage to mouse photoreceptors. *Mamm Genome*. 2000;11: 422–427.
23. Wenzel A, Reme CE, Williams TP, Hafezi F, Grimm C. The Rpe65 Leu450Met variation increases retinal resistance against light-induced degeneration by slowing rhodopsin regeneration. *J Neurosci*. 2001;21:53–58.
24. Kranich H, Bartkowski S, Denton MJ, et al. Autosomal dominant "sector" retinitis pigmentosa due to a point mutation predicting an Asn-15-ser substitution of rhodopsin. *Hum Mol Genet*. 1993;2:813–814.
25. Li Z, Jacobson SG, Milam AH. Autosomal dominant retinitis pigmentosa caused by the threonine-17-methionine rhodopsin mutation: retinal histopathology and immunocytochemistry. *Exp Eye Res*. 1994;58:397–408.
26. Moore A, Fitzke F, Kemp C, et al. Abnormal dark-adaptation kinetics in autosomal dominant sector retinitis-pigmentosa due to rod opsin mutation. *Br J Ophthalmol*. 1992;76:465–469.
27. Fishman GA, Stone EM, Sheffield VC, Gilbert LD, Kimura AE. Ocular findings associated with rhodopsin gene codon 17 and codon 182 transition mutations in dominant retinitis pigmentosa. *Arch Ophthalmol*. 1992;110:54–62.
28. Napier ML, Durga D, Wolsley CJ, et al. Mutational analysis of the rhodopsin gene in sector retinitis pigmentosa. *Ophthalmic Genet*. 2015;36:239–243.
29. Rivera-De la Parra D, Cabral-Macias J, Matias-Florentino M, Rodriguez-Ruiz G, Robredo V, Zenteno JC. Rhodopsin p.N78I dominant mutation causing sectorial retinitis pigmentosa in a pedigree with intrafamilial clinical heterogeneity. *Gene*. 2013; 519:173–176.
30. Katagiri S, Hayashi T, Akahori M, et al. RHO mutations (p.W126L and p.A346P) in two Japanese families with autosomal dominant retinitis pigmentosa. 2014;2014:210947.
31. Mendes HF, van der Spuy J, Chapple JP, Cheetham ME. Mechanisms of cell death in rhodopsin retinitis pigmentosa: implications for therapy. *Trends Mol Med*. 2005;11:177–185.
32. Haeri M, Knox BE. Rhodopsin mutant P23H destabilizes rod photoreceptor disk membranes. *PLoS One*. 2012;7:e30101.
33. Samardzija M, Wenzel A, Naash M, Remé CE, Grimm C. Rpe65 as a modifier gene for inherited retinal degeneration. *Eur J Neurosci*. 2006;23:1028–1034.
34. Sakami S, Kolesnikov AV, Kefalov VJ, Palczewski K. P23H opsin knock-in mice reveal a novel step in retinal rod disc morphogenesis. *Hum Mol Genet*. 2014;23:1723–1741.
35. Chiang W-C, Kroeger H, Sakami S, et al. Robust endoplasmic reticulum-associated degradation of rhodopsin precedes retinal degeneration. *Mol Neurobiol*. 2015;52:679–695.

36. Yao J, Qiu Y, Frontera E, et al. Inhibiting autophagy reduces retinal degeneration caused by protein misfolding. *Autophagy*. 2018;14:1226–1238.
37. Sancho-Pelluz J, Tosi J, Hsu C, Lee F, Wolpert K. Mice with a D190N mutation in the gene encoding rhodopsin: a model for human autosomal-dominant. *Mol Med*. 2012;18:549–555.
38. White DA, Hauswirth WW, Kaushal S, Lewin AS. Increased sensitivity to light-induced damage in a mouse model of autosomal dominant retinal disease. *Invest Ophthalmol Vis Sci*. 2007;48:1942–1951.
39. Cideciyan AV, Hood DC, Huang Y, et al. Disease sequence from mutant rhodopsin allele to rod and cone photoreceptor degeneration in man. *Proc Natl Acad Sci U S A*. 1998;95:7103–7108.
40. Narayan DS, Wood JPM, Chidlow G, Casson RJ. A review of the mechanisms of cone degeneration in retinitis pigmentosa. *Acta Ophthalmol*. 2016;94:748–754.
41. Campochiaro PA, Mir TA. The mechanism of cone cell death in retinitis pigmentosa. *Prog Retin Eye Res*. 2018;62:24–37.
42. Yu DY, Cringle S, Valter K, Walsh N, Lee D, Stone J. Photoreceptor death, trophic factor expression, retinal oxygen status, and photoreceptor function in the P23H rat. *Invest Ophthalmol Vis Sci*. 2004;45:2013–2019.
43. Elachouri G, Lee-Rivera I, Clérin E, et al. Thioredoxin rod-derived cone viability factor protects against photooxidative retinal damage. *Free Radic Biol Med*. 2015;81:22–29.
44. Morrissette D, Mehr E, Keswick C, Lee P. Users' and nonusers' evaluations of the CPF 550 lenses. *Am J Optom Physiol Opt*. 1984;61:704–710.
45. Neitz J, Carroll J, Yamauchi Y, Neitz M, Williams DR. Color perception is mediated by a plastic neural mechanism that is adjustable in adults. *Neuron*. 2002;35:783–792.
46. Bailes H, Lucan R. Human melanopsin forms a pigment maximally sensitive to blue light (lambda max = 479 nm) supporting activation of Gq/11 and Gi/o signalling cascades. *Proc Natl Acad Sci U S A*. 2013;280:1–9.
47. Benarroch EE. The melanopsin system: phototransduction, projections, functions, and clinical implications. *Neurology*. 2011;76:1422–1427.
48. Kessel L, Lundeman JH, Herbst K, Andersen TV, Larsen M. Age-related changes in the transmission properties of the human lens and their relevance to circadian entrainment. *J Cataract Refract Surg*. 2010;36:308–312.
49. Kessel L, Siganos G, Jørgensen T, Larsen M. Sleep disturbances are related to decreased transmission of blue light to the retina caused by lens yellowing. *Sleep*. 2011;34:1215–1219.
50. Kim YH, Jung KI, Song CH. The effect of cataract on sleep time and quality in late adulthood. *Aging Clin Exp Res*. 2012;24:663–668.
51. Giménez MC, Beersma DGM, Bollen P, Van Der Linden ML, Gordijn MCM. Effects of a chronic reduction of short-wavelength light input on melatonin and sleep patterns in humans: evidence for adaptation. *Chronobiol Int*. 2014;31:690–697.

Investigative Ophthalmology & Visual Science